Neurotoxicity Research (2019) 36:117–131
https://doi.org/10.1007/s12640-019-00043-9

ORIGINAL ARTICLE

# Suppressing nNOS Enzyme by Small-Interfering RNAs Protects SH-SY5Y Cells and Nigral Dopaminergic Neurons from 6-OHDA Injury

Ricardo Titze-de-Almeida[1] · Simoneide S. Titze-de-Almeida[1] · Nadia Rubia Ferreira[2] · Caroline Fontanari[3] · Lúcia Helena Faccioli[3] · Elaine Del Bel[2,4]

Received: 26 February 2019 / Revised: 27 March 2019 / Accepted: 4 April 2019 / Published online: 30 April 2019
© Springer Science+Business Media, LLC, part of Springer Nature 2019

## Abstract

Nitric oxide (NO) has chemical properties that make it uniquely suitable as an intracellular and intercellular messenger. NO is produced by the activity of the enzyme nitric oxide synthases (NOS). There is substantial and mounting evidence that slight abnormalities of NO may underlie a wide range of neurodegenerative disorders. NO participates of the oxidative stress and inflammatory processes that contribute to the progressive dopaminergic loss in Parkinson's disease (PD). The present study aimed to evaluate in vitro and in vivo the effects of neuronal NOS-targeted siRNAs on the injury caused in dopaminergic neurons by the toxin 6-hidroxydopamine (6-OHDA). First, we confirmed (immunohistochemistry and Western blotting) that SH-SY5Y cell lineage expresses the dopaminergic marker tyrosine hydroxylase (TH) and the protein under analysis, neuronal NOS (nNOS). We designed four siRNAs by using the BIOPREDsi algorithm choosing the one providing the highest knockdown of nNOS mRNA in SH-SY5Y cells, as determined by qPCR. siRNA 4400 carried by liposomes was internalized into cells, caused a concentration-dependent knockdown on nNOS, and reduced the toxicity induced by 6-OHDA ($p < 0.05$). Regarding in vivo action in the dopamine-depleted animals, intra-striatal injection of siRNA 4400 at 4 days prior 6-OHDA produced a decrease in the rotational behavior induced by apomorphine. Finally, siRNA 4400 mitigated the loss of TH(+) cells in substantia nigra dorsal and ventral part. In conclusion, the suppression of nNOS enzyme by targeted siRNAs modified the progressive death of dopaminergic cells induced by 6-OHDA and merits further pre-clinical investigations as a neuroprotective approach for PD.

**Keywords** Nitric oxide · Nitric oxide synthases · siRNAs · 6-OHDA · Parkinson's disease · Tyrosine hydroxylase

## Introduction

Nitric oxide (NO) is the only endogenous molecule that functions as a hormone, reactive oxygen species (ROS), neurotransmitter, constitutive mediator, inducible mediator, cytoprotective, and cytotoxic molecule (Del Bel et al. 2005; Del-Bel et al. 2011). Oxidative stress is a cell process mediated by ROS that plays a critical role in neurodegenerative disorders including Parkinson's disease (PD) (Jimenez-Jimenez et al. 2016; Przedborski 2005). NO is among the ROS molecules involved in neuron damage due to inhibition of respiratory chain enzymes, injury to DNA strands, generation of toxic hydroxyl radicals, and peroxynitrite (Brown 2010; Ebadi and Sharma 2003; Hunot et al. 1996).

Nitric oxide synthases (NOS) comprise a family of enzyme isoforms that generate NO (Alderton et al. 2001). The neuronal NOS (nNOS, NOS1) is constitutively expressed in neuron, while endothelial NOS (eNOS, NOS3) was first reported in endothelial cells. The inducible NOS (iNOS, NOS2) is an isoform expressed by different cells mainly under inflammatory conditions (Calabrese et al. 2007; Moncada and Bolanos 2006). Growing evidence stand NOS enzymes are engaged in dopaminergic neuron loss and brain neuroinflammation (Gaki and

Simoneide S. Titze-de-Almeida and Nádia Rubia Ferreira contributed equally to this work.

✉ Elaine Del Bel
eadelbel@usp.br

[1] Technology for Gene Therapy Laboratory, Central Institute of Sciences, University of Brasília–FAV, Brasília, DF 70910-900, Brazil

[2] Department of Basic and Oral Biology, Dental School, University of São Paulo (USP), Ribeirão Preto, SP 14040-904, Brazil

[3] Department of Clinical Analyses, Toxicology and Bromatology, School of Pharmaceutical Sciences of Ribeirão Preto, University of São Paulo, Ribeirão Preto, SP 14040-903, Brazil

[4] Center for Interdisciplinary Research on Applied Neurosciences (NAPNA), University of São Paulo (USP), São Paulo, SP, Brazil

Papavassiliou 2014; Hara and Snyder 2007; Kavya et al. 2006). The logical rationale was that a blockade of NOS enzymes would be neuroprotective. Our group addressed such question and found that a nonselective NOS inhibition with NG-nitro-L-arginine (L-NOARG) reduced the nigrostriatal damage caused by 6-hidroxydopamine (6-OHDA) (Gomes and Del Bel 2003; Gomes et al. 2008). Indeed, a preferential blockade of nNOS with 7-nitroindazole (7-NI) also attenuated both the dopamine neuron loss and behavioral deficits caused by 6-OHDA (Haik et al. 2008). Finally, we reported a neuroprotective effect of 7-NI on SH-SY5Y dopaminergic cell damaged by another chemical insult, MPP(+) (1-methyl-4-phenylpyridinium) plus interferon gamma (Titze-de-Almeida et al. 2014).

While those findings confirmed a role for nNOS in dopaminergic neurodegeneration, they also highlighted this enzyme as a potential target for PD therapy. Drugs capable of suppressing nNOS hold potential for controlling disease progression, an unmet medical need (Dunkel et al. 2012). Many new selective nNOS inhibitors are available, with reduced off-target effects related to other isoforms (i.e., hypertension caused by eNOS suppression) and favorable pharmacokinetics to access brain tissues (Mukherjee et al. 2014; Zhou and Zhu 2009). Another promising approach to suppress a desired protein is to silence its expression at a posttranscriptional level, a strategy available only after RNAi discovery (Fire et al. 1998). Nowadays, ten RNAi-based drugs have reached phase II human clinical trials for treating various diseases (Titze-de-Almeida et al. 2017). Regarding nNOS enzyme, we have successfully silenced this target by using siRNAs in both in vitro and in vivo studies (Castania et al. 2017; Titze-de-Almeida et al. 2014). Silencing efficiency of the proposed nNOS-targeted siRNAs can be improved through chemical changes in oligonucleotides or by new carriers dedicated to brain delivery (Soto-Sanchez et al. 2015; Titze-de-Almeida et al. 2017).

siRNAs designed to silence nNOS expression may provide a valuable tool for studies on dopaminergic neurodegeneration. Among the advantages of silencing nNOS at a posttranscriptional level over the classical nNOS inhibitors are the inhibition of a specific enzyme isoform and the examination of effects only on the newly synthesized enzyme, without affecting the activity of corresponding proteins already expressed in neuron cells. The aim of present work was to investigate nNOS suppression by small-interfering RNAs (siRNAs) in both in vitro and in vivo 6-OHDA-induced injury model.

## Material and Methods

### Cell Culture

This study used the human neuroblastoma cell line SH-SY5Y (CRL-2266®; American Type Culture Collection, Manassas, VA, USA). Culture medium was Dulbecco's modified Eagle's medium (DMEM)/F12 (Gibco; Thermo Fisher Scientific, Inc., Waltham, MA, USA) containing 10% fetal bovine serum (Gibco; Thermo Fisher Scientific, Inc.), 1% Glutamax (Gibco; Thermo Fisher Scientific, Inc.), streptomycin/penicillin/amphotericin (Sigma-Aldrich; Merck Millipore; Darmstadt, Germany). Culture flasks remained at 37 °C in a humidified atmosphere containing 5% $CO_2$ and 95% air.

### Cytotoxicity Assay on 6-OHDA-Injured SH-SY5Y Cells

Cell cytotoxicity was measured by using the MTT (3-(4,5-Dimethylthiazol-2-yl)-2,5-Diphenyltetrazolium Bromide) quantitative colorimetric assay (Titze-de-Almeida et al. 2014; Vistica et al. 1991). Briefly, 50 μL of MTT-labeling reagent (0.5 mg/mL) was added to each well, and the plate was maintained at 37 °C in a humidified atmosphere of 5% $CO_2$ and 95% air for an additional 3-h period. The insoluble formazan was dissolved by dimethyl sulfoxide (DMSO), and the MTT reduction was measured at 595 nm in a SpectraMax M2 (Molecular Devices, USA). Injured groups were exposed to increasing concentrations of 6-OHDA (10, 15, 20, 25, 30, 35 μM) for 24 h. All assays included non-injured control cells. Experiments were carried out in triplicate, in 3–5 independent assays.

### Immunodetection of Tyrosine Hydroxylase and nNOS Proteins in SH-SY5Y Cells and Tissue Samples

Immunocytochemical analysis of TH and nNOS were performed with dopaminergic neuron-like SH-SY5Y cell lineage. Cells ($2 \times 10^5$) were cultured on coverslips in 24-well plates, then fixed for 15 min in 4% paraformaldehyde. Cells were incubated overnight with the primary antibody raised against TH or nNOS (TH: 1/1000, Pel Freez Biologicals, USA; or nNOS: 1/1000, Emson—see Herbison et al. 1996 (Herbison et al. 1996)). We proceed to the streptavidin–biotin immunoperoxidase detection method according to manufacturer's instructions (Vectastain ABC kit, Vector, Burlingame, CA). Immunopositive cells were visualized by addition of the chromogen 3,3′-diaminobenzidine (DAB; Sigma, 1 mg/mL) and hydrogen peroxide (0.2%), providing a brown reaction product. Coverslips were mounted for microscopic analyses. Immunohistochemistry detection of TH and nNOS in brain tissue samples employed the same primary antibodies and followed previously described protocols (Douhou et al. 2002; Gomes et al. 2008; Herbison et al. 1996). Densitometry of TH+ cells in substantia nigra (SN) was performed as previously described (Gomes et al. 2008). Incubations without the primary antibody were

used as negative controls. Tissues of every experimental group were always processed in the same assay. Finally, we executed histological analysis on positively stained dopaminergic neurons. TH-positive cells in SN were counted bilaterally by using a microscope (Nikon) connected to an image analysis system (Image J software 1.46J; Rasband, National Institutes of Health, Bethesda, MD). Results were expressed as the mean density of positive neurons in each brain side. Labeling of TH-positive neurons was accessed by optical density, measuring average pixel optical density over cell body and network. Counts and measurements of 3–4 sections were averaged to generate a mean value per rat. The background was subtracted from all subsequent measurements.

## Western Blotting

For immunoblotting assays in SH-SY5Y cell groups, we used the TH primary antibody described above (Pel Freez Biologicals, USA) and a mouse monoclonal anti-nNOS (1:1000, BD Biosciences, USA), following a previously described protocol (Grant et al. 2002). Regarding rat brain tissues, Western blotting was carried out according to previously published study (Padovan-Neto et al. 2011). For both samples, we employed the mouse monoclonal anti-ß-actin (1:5000, Santa Cruz Biotechnology, USA) for experimental control. Briefly, the striatum was dissected, frozen in liquid nitrogen (− 196 °C) and stored at − 80 °C. Tissue homogenates were centrifuged (10,000 rpm for 25 min at 4 °C) and supernatants recovered to determine protein concentration by Bradford assay (Bio-Rad Protein assay, Bio-Rad, Germany). A total of 30 μg protein was resolved by sodium dodecyl sulfate polyacrylamide gel electrophoresis (8% SDS-PAGE) and transferred to a nitrocellulose membrane by using a semi-dry method. Membranes were incubated at 4 °C overnight with the primary antibodies described above. For detection, we used an HRP-conjugated secondary antibody. Bands were visualized by enhanced chemiluminescence (ECL, Amersham, UK). Each experiment was performed at least three times with similar results.

## Identifying RNAi Targets in nNOS mRNA

This study used the BIOPREDsi algorithm to find targets for RNAi in nNOS mRNA (Huesken et al. 2005). Based on artificial neural networks, the method has presented a superior performance for designing siRNAs as found in a comparative study (Matveeva et al. 2007). BIOPREDsi identified ten targets for RNAi in the rat nNOS mRNA with scores ranging from 0.888739 to 0.86052 (Table 1). Algorithms in general present ≈ 0.5 correlation coefficient between theoretical prediction and experimental functionality (Birmingham et al. 2007); thus, we selected four sequences to obtain at least two siRNAs that efficiently knock down nNOS. The four targets followed consensual rules for siRNA design: (1) highest score in algorithm prediction (i.e., BIOPREDsi ranking); (2) G + C content between 30 and 60%; (3) siRNA target within mRNA coding sequence region; (4) target sequence coded in distinct exon to the other selected target, allowing a spatially distributed RNAi in nNOS mRNA; (5) high conservation (i.e., lowest mutability) among rodent and human species, enabling long-term experimental needs with orthologous siRNAs; (6) targeted sequence identical among the main nNOS isoforms and splice variants; (7) low potential to induce off-target effects, as checked by alignment algorithms as described below (Birmingham et al. 2007; Hajeri and Singh 2009; Reynolds et al. 2004). We also employed a second siRNA finder named Designer of Small Interfering RNA algorithm (DSIR) as an additional criteria to the BIOPREDsi ranking (Vert et al. 2006).

## Genetic Variability in nNOS mRNA Transcript Variants

The nucleotide sequences within mRNA's siRNA targets are a determinant factor for gene silencing by RNAi (Titze-de-Almeida et al. 2017). Thus, we examined nNOS (NOS1) sequences of human and rat species annotated in NIH/NCBI Genebank® to check whether nNOS mRNA isoforms and variants have no mutations in the four BIOPREDsi siRNA targets. The human nNOS mRNA sequences evaluated were XM_017019345.1 (transcript variant X1), XM_011538398.2 (transcript variant X2), XM_017019346.1 (transcript variant X3), XM_017019347.1 (transcript variant X4), NM_000620.4 (transcript variant 1), NM_001204218.1 (transcript variant 2; nNOS *mu*), NM_001204213.1 (transcript variant 3; TnNOS, nNOS *gamma*), and NM_001204214.1 (transcript variant 4; TnNOSb, nNOS *gamma*). Regarding rat sequences, this study evaluated the following variants: NM_052799.1 (NOS1), XM_017598256.1 (transcript variant X1), and XM_017598257.1 (transcript variant X2). To examine potential mutations in the human and rat nNOS siRNA target sequences, we used the multiple alignment program Clustal Omega available at http://www.ebi.ac.uk/Tools/msa/clustalo/. Acceptable siRNAs must target nNOS sequences without any mutation among transcript variants.

## siRNA Transfection Rates in SH-SY5Y Cells

The efficiency of cationic liposomes in transfecting SH-SY5Y with synthetic siRNAs was first examined by fluorescence microscopy. Cells received 150 pmol of

**Table 1** siRNA target sequences in nNOS mRNA

| Rank | siRNA-target (start position at rat nNOS mRNA NM_052799.1) | Biopredsi score | siRNA antisense strand (guide) 5′–3′ | siRNA sense strand (passenger) 5′–3′ | G + C content (%) | Mismatches to human nNOS CCDS41842.1 | Mismatches to the mouse nNOS CCDS19606.1 | DSIR prediction Rank (% score) |
|---|---|---|---|---|---|---|---|---|
| 1 | 3987 | 0.888739 | UUGGAUGUCAAAUUGUCGCTG | GCGACAAUUUGACAUCCAATT | 40.5 | 2 | 0 | 1 (104.4%) |
| 2 | 2990 | 0.880512 | UUGAAGACUUUCUUGGCCCAG | GGGCCAAGAAAGUCUUCAATT | 45.2 | 1 | 1 | negative[a] |
| 3 | 4148 | 0.873566 | UAUUUCUUUGGCCUGUCCGGT | CGGACAGGCCAAAGAAAUATT | 45.2 | 5 | 1 | negative[a] |
| 4 | 4400 | 0.871441 | UUGGUCACUUCAUACGUUCTG | GAACGUAUGAAGUGACCAATT | 40.5 | 3 | 1 | 25 (95.7%) |
| 5 | 2063 | 0.871382 | UGUUUGAUGAAGGACUCCGTG | CGGAGUCCUUCAUCAAACATT | 45.2 | 3 | 1 | 35 (94.0%) |
| 6 | 3330 | 0.866846 | UUCAAUGAGUGCAUUCACGAG | CGUGAAUGCACUCAUUGAATT | 40.5 | 4 | 0 | 29 (94.7%) |
| 7 | 87 | 0.864471 | UUCCAUGGUAUCUGUGUCCTT | GGACACAGAUACCAUGGAATT | 42.9 | n/a | n/a | negative[a] |
| 8 | 767 | 0.863301 | UUCAUCUCUGCUUUGGCUGGT | CAGCCAAAGCAGAGAUGAATT | 45.2 | 2 | 0 | negative[a] |
| 9 | 1604 | 0.860640 | UGCUGUAUACAGAUCUCCGTG | CGGAGAUCUGUAUACAGCATT | 45.2 | 3 | 1 | 38 (93.9%) |
| 10 | 607 | 0.860520 | UAGCUUGGGAGACUGAGCCAG | GGCUCAGUCUCCCAAGCUATT | 54.8 | 4 | 2 | 3 (100.1%) |

[a] Negative: target not predicted by DSIR algorithm; n/a: human and mouse coding sequences not available at this position

AlexaFluor488-labeled siRNAs mixed with Lipofectamine (Lipofectamine® 2000 Transfection Reagent, Invitrogen, Carlsbad, CA, USA), following manufacturer's instructions. Green fluorescence inside cell cytoplasm indicated a successful transfection of labeled siRNAs, as examined at 24 h. Indeed, the number of transfected cells at three increased concentrations of siRNAs (75, 150, and 300 pmol) was quantified by using a previously reported flow cytometry assay (Sales et al. 2016).

## Cell Transfection, RNA Extraction, Reverse Transcription Real-Time Quantitative Polymerase Chain Reaction

First, transfections with siRNAs were carried out with Lipofectamine (Lipofectamine® 2000 Transfection Reagent, Invitrogen, Carlsbad, CA, USA) and Opti-Mem I (Invitrogen, Carlsbad, CA, USA), according to the manufacturer's instructions. The SH-SY5Y dopaminergic cells received the siRNAs 767, 2063, 3987, or 4400 at three different amounts (75, 150, and 300 pmol) for 24 h. Also, the dose of 150 pmol was tested at time points 4 h, 24 h, and 48 h. Total RNA was extracted with a commercial kit (RNeasy® Plus Mini Kit, Qiagen, Hilden, Germany) and quantified by fluorometry (Qubit®, Invitrogen). The RNA integrity was analyzed by agarose gel electrophoresis, visualized under UV light. The sample purity was considered acceptable for RNA/protein ratios above 1.8. cDNA was synthesized from 500 ng total RNA by using random primers (SuperScript First-Strand Synthesis System for RT-PCR, Invitrogen). We performed the RT-qPCR reaction in a 7500 Fast Real-Time PCR (Applied Biosystems, Carlsbad, CA, USA). The primer sequences for nNOS amplification were forward, 5′-GGTG GAGATCAATATCGCGGTT-3′ and reverse, 5′-CCGG CAGCGGTACTCATTCT-3′ (Dotsch et al. 2000). For the housekeeping gene, we used the following GC-rich promoter binding protein 1 (GPBP1) primers: forward, 5′-TCACTTGAGGCAGAACACAGA-3′ and reverse, 5′-AGCACATGTTTCATCATTTTCAC-3′ (Kwon et al. 2009). Intercalation of the fluorescent dye SYBR Green was applied to detect amplification products. Briefly, the reaction mix contained 5.0-μL Fast SYBR Green Master mix (Applied Biosystems), 2.0 μL of cDNA diluted 1:10, 0.4 μL each primer (sense and antisense; 10 pmol/μL), and Milli-Q pure water up to 10.0 μL. The PCR program included an initial denaturation at 95 °C for 5 min, followed by 40 cycles of amplification (95 °C for 1 min, 60 °C for 1 min). Each run was carried out in triplicate. The assay included negative reverse transcription (non-template) controls. Finally, we employed the delta Ct ($2^{-\Delta\Delta Ct}$) relative quantification method to express the RNAi effects on nNOS mRNA content (Livak and Schmittgen 2001).

## Intra-striatal Injections of nNOS-Targeted siRNAs and 6-OHDA

In vivo assays used adult male *Wistar* rats (200–250 g), housed in groups of five per cage in a temperature-controlled room (23 °C), under 12-h light/dark cycle, with food and water ad libitum. The experiments followed the principles and procedures described in the Guidelines for the Care and Use of Mammals in Neuroscience and Behavioral Research (ILAR, USA). A total of 30 animals were organized in the following experimental groups: sham-operated ($n = 10$), injected with siRNA 4400 ($n = 10$), and injected with the negative control siRNA ($n = 10$). Rats were submitted to stereotaxic surgery as previously described (Padovan-Neto et al. 2009). Briefly, on day 1, the animals were anesthetized with tribromoethanol (0.25 mg/kg i.p., Sigma-Aldrich, St. Louis, MO, USA) and fixed on a stereotaxic frame (David-Kopf) with the incisor bar 5 mm above the interaural line. Then, rats received four intrastriatal injections of 300 pmol siRNA 4400 or the negative scramble control siRNA (All stars®, Qiagen, Valencia, CA, USA) mixed with Lipofectamine (Lipofectamine 2000 Transfection Reagent, Invitrogen, Carlsbad, CA, USA), each injection was conducted in one of the following coordinates: (1) A: + 1.3 L: − 2.6 D: − 5.0; (2) A + 0.4 L: − 3.2 D: − 5.0; (3) A: − 0.4 L: − 4.2 D: − 5.0; (4) A: − 1.3 L: − 4.5 D: − 5.0 from Bregma, according to the atlas of Paxinos and Watson (Paxinos and Watson 2005). The siRNA 4400 was infused at the rate of 1 μL/min with an infusion pump (Scientific, USA). The needle was left in place for an additional 3 min before withdrawal, to prevent reflux. On day 5, we proceed the striatal lesion with 6-OHDA (4 × 7 μg/2 μL of saline containing 0.02% ascorbic acid) microinjection into the right striatum at the same four coordinates, as previously reported (Gomes et al. 2008). To limit the damage in noradrenergic neurons, desipramine hydrochloride (25 mg/kg i.p., Sigma-Aldrich, St. Louis, MO, USA) and pargyline (40 mg/kg, Sigma-Aldrich, St. Louis, MO, USA) were administered 30 min before 6-OHDA injection. Sham-operated animals were submitted to the same procedure, receiving saline microinjection. Rats were placed in clean cages on warming pads to recover from the surgery, after which they were returned to group housing.

## Rotational Behavior Test

Rotational behavior was examined at 24 days after 6-OHDA intra-striatal injection, as previously described

(Padovan-Neto et al. 2009). Briefly, animals were first placed in a 40-cm-diameter bowl surrounded by a 16-cm wall and allowed to acclimate to the environment for 10 min. They received apomorphine (0.5 mg/kg; s.c.) and the total number of full contra-lateral rotations—defined as a complete 360° turns away from the lesioned side of the brain—were counted for 45 min.

### Statistical Analysis

Statistical package for social sciences (SPSS) version 17 was employed to analyze our data. Results were expressed as means ± standard error of the means (SEM). One-way analysis of variance (ANOVA) with Tukey's post hoc test was used for testing intergroup differences. Differences between paired groups were analyzed by the Student's *t* test. *P* values of $< 0.05$ were considered significant.

## Results

### Tyrosine Hydroxylase-Positive SH-SY5Y Cells Express nNOS Enzyme and Are Susceptible to 6-OHDA

Our first attempt was to evaluate the potential of SH-SY5Y cell line for modeling dopaminergic neuron injury. This cell line must show the following characteristics: (i) to be positive for TH, (ii) to be positive for nNOS, and (iii) to be susceptible to 6-OHDA neurotoxin.

SH-SY5Y cells presented a phenotype of a dopaminergic neuron as evidenced by the detection of TH protein immunocytochemistry (Fig. 1I). The intensity of TH signal reduced progressively according to serial dilutions of primary antibody 1:500, 1:1000, 1:2000, and 1:4000 (Fig. 1IB–E). Western blotting analysis confirmed SH-SY5Y cell expression of the enzyme, regardless they were treated or not with retinoic acid (Fig. 1II, lanes 3 and 4). We included samples of mesencephalic rat brain tissue as positive controls (Fig. 1II, lanes 1 and 2). Therefore, the results confirmed the dopaminergic feature of SH-SY5Y cells.

Secondly, we examined the expression of nNOS enzyme. Immunocytochemistry assays revealed a nNOS-positivity in cells exposed to serial concentration of the primary antibody at 1:1000–1:9000 (Fig. 1IIIB–E). Expression of nNOS was confirmed by Western blotting in SH-SY5Y cells (Fig. 1IV lanes 2–5), in comparison with mesencephalic positive control samples (Fig. 1IV lane 1). Retinoic acid caused no changes in nNOS expression (Fig. 1IV lanes 2–4 vs. lane 5).

Finally, we tested if our in vitro model based on TH(+) cells expressing nNOS was vulnerable to 6-OHDA. We confirmed that 6-OHDA neurotoxin induces a dose-dependent damage in SH-SY5Y cells. Cytotoxicity increased from 25 to ≈ 100% for 6-OHDA concentrations of 5 μM and 30–35 μM, respectively (Fig. 1V). As 6-OHDA 15 μM was of intermediary toxicity (≈ 58%), we chose this 6-OHDA concentration for further assays regarding nNOS gene silencing.

### Targets for RNAi in nNOS mRNA

The BIOPREDsi algorithm successfully identified siRNA targets in nNOS mRNA. The three sequences first selected for this study start at nucleotides 3987 (top ranked, score 0.888739), 4400 (rank 4, score 0.871441), and 2063 (rank 5, score 0.871382), which were named 3987, 4400, and 2063 for simplicity. Sequences at nucleotides 2990 and 4148 (ranks 2 and 3) received less priority than 4400 and 2063 because they were negative for DSIR algorithm (Table 1) (Vert et al. 2006). Finally, we included a siRNA that targets a sequence at nucleotide 767, which is present in all human nNOS transcript variants except the 3 and 4 (nNOS *gamma*) that spares exon 2 (Fig. 2). Thus, the four selected RNAi targets (767, 2063, 3987, and 4400) were sequences of nNOS transcript variants 2, X1, X2, X3, and X4. These siRNA targets are also present in the rat nos1 and variants X1 and X2 (Fig. 3). We must remark the targets 767, 2063, 3987, and 4400 are spatially distributed in nNOS mRNA, regarding coding sequences of exons 2, 12, 25, and 28, respectively (Fig. 2). Positions of nNOS siRNA-target sequences in the rat and human mRNA and the mutated nucleotides between these species are shown in Table 2.

### Transfection of siRNAs in SH-SY5Y Cells

nNOS-targeted siRNAs carried by cationic liposomes were internalized by SH-SY5Y cells in culture. As shown in Fig. 4a (B and B′; yellow arrows), some Alexa Fluor 488-labeled siRNAs were found in cell cytoplasm. Non-transfected siRNAs remain in regions of culture flasks without growing cells as pointed by red arrows. Indeed, a flow cytometry assay was used to quantify transfection efficiency. The method revealed a concentration-dependent increase in the number of transfected SH-SY5Y cells regarding the amount of siRNA employed in transfections (Fig. 4c–e). The number of Alexa Fluor 488-positive cells (170.4, 224.6, and 290.9) increased according to the following siRNA concentrations, 75, 150, and 300 pmol, respectively.

### Concentration- and Target-Dependent Knockdown of nNOS mRNA

All four sequences predicted by the BIOPREDsi algorithm, 767, 2063, 3987, and 4400, were functional targets for nNOS gene silencing. Transfections with 75, 150, and 300 pmol of siRNAs caused a concentration-dependent decrease in nNOS mRNA content of SH-SY5Y cells, as shown in Fig. 5a–c.

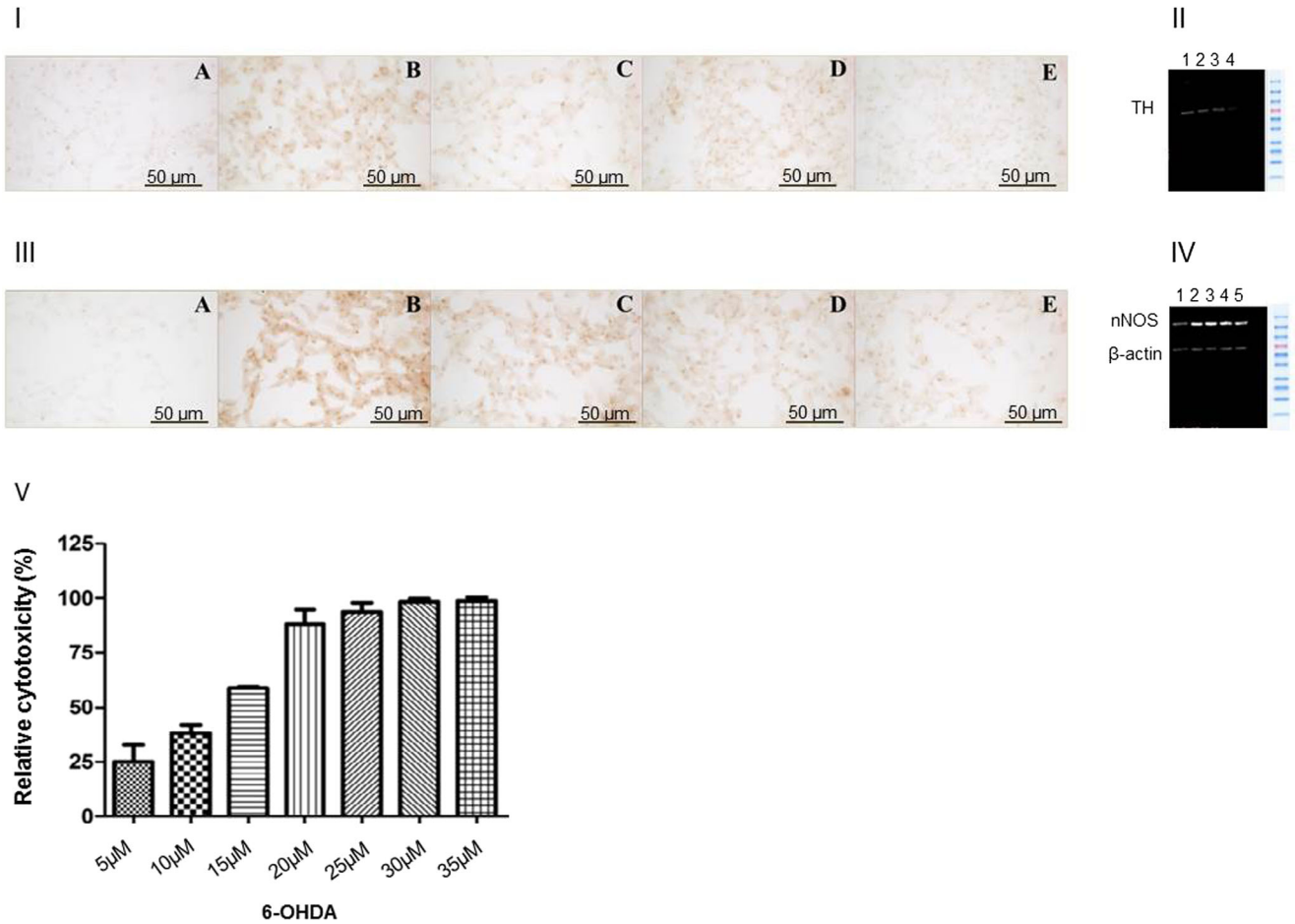


**Fig. 1** TH and nNOS expression in SH-SY5Y lineage and cytotoxicity assay of 6-OHDA-injured cells. **I** Titulation of TH antibody in SH-SY5Y cells (A: negative control; B: 1:500; C: 1:1000; D 1:2000; E: 1:4000). **II** Western blotting of TH (≈ 60 kDa)-mesencephalus (lanes 1–2); SH-SY5Y cells treated with retinoic acid (lane 3); sham-treated SH-SY5Y cells (lane 4). **III** Titulation of nNOS antibody (A: negative control; B: 1:000; C: 1:3000; D: 1:6000; E: 1:9000). **IV** Western blotting of nNOS (155 kDa)-mesencephalus (lane 1); retinoic acid-treated SH-SY5Y cells (lanes 2–3); sham-treated SH-SY5Y cells (lanes 4–5); β-actin (45 kDa). **V** Concentration-dependent cytotoxicity of 6-OHDA on SH-SY5Y cells

However, silencing efficiency differed among siRNA-targets. Sequence 4400 offered the highest knocking down effect, reaching 0.7-, 0.6-, and 0.5-fold decrease in nNOS content at 75, 150, and 300 pmol siRNA, respectively. The difference was statistically significant in comparison with the targets 767 and 2063, at 75 pmol and 300 pmol (Fig. 5a–c; $P < 0.05$). Silencing activity of target 4400 was also superior regarding different time points post transfection: 4 h, 24 h, and 72 h. As shown in Fig. 5d, f, target 4400 provided a significant higher silencing effect at 4 h and 48 h as compared with targets 767 and 2063 ($P < 0.05$). Based on those results, we selected target 4400 for all further assays of this study.

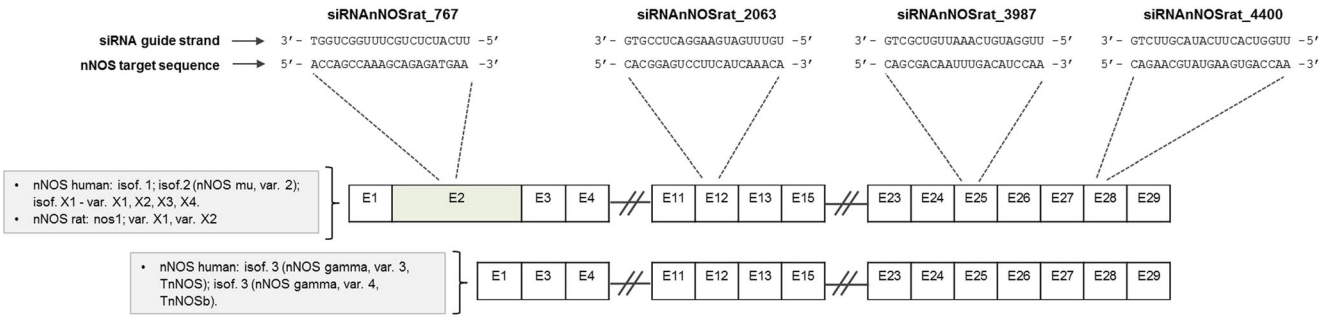


**Fig. 2** Distribution of siRNA targets in nNOS coding exons**.** nNOS-target sequences are spatially distributed along with nNOS mRNA coding sequences, as follows: siRNAnNOSrat_767, exon 2 (E2); siRNAnNOSrat_2063, exon 12 (E12); siRNAnNOSrat_3987, exon 25 (E25); siRNAnNOSrat_4400, exon 28 (E28). Orthologous human siRNAs follow the same distribution

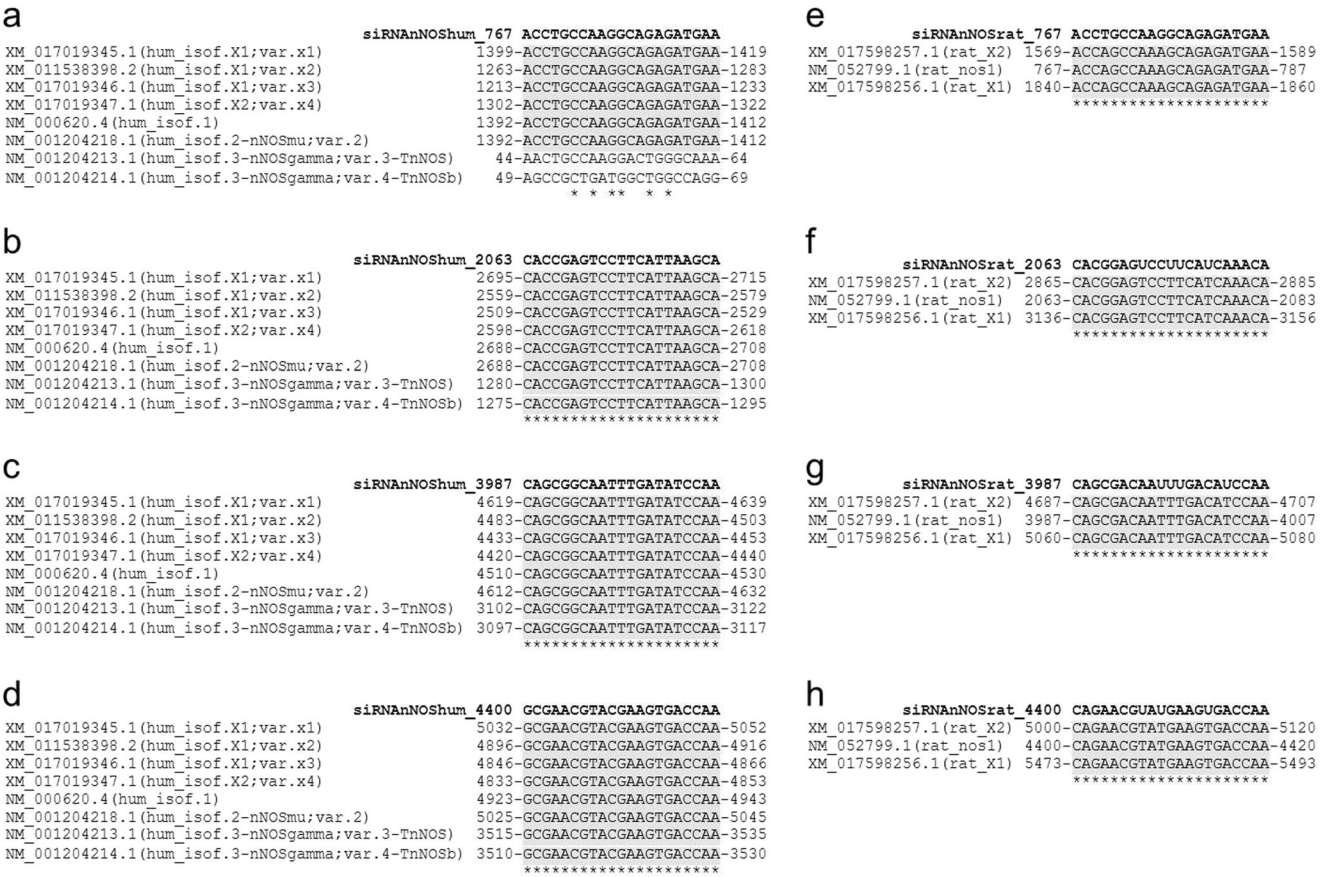


**Fig. 3** siRNA targets in human and rat nNOS isoforms and variants. **a-d** Alignment between siRNAnNOShuman_767, _2063, _3987, _4400 and sequences of human nNOS isoforms (isof.) and variants (var.). siRNAnNOShuman_767 showed alignment with all human nNOS isoforms except isof. 3 (nNOS gamma; NM_001204213.1 and NM_001204214.1) due the lack of exon 2 (**a**). All other human siRNAs (siRNAnNOShum_2063, _3987, and _4400) were fully aligned with all nNOS isoforms and variants. **e-h** Alignment of siRNAnNOSrat_767, _2063, _3987, _4400 to nNOS rat mRNA sequences. All rat siRNAs (siRNAnNOSrat_767, _2063, _3987, and _4400) showed full alignment

## Knocking Down of nNOS Protein and the Neuroprotective Effect in 6-OHDA Injured Cells

The silencing effects of siRNAs targeting sequence 4400 also occurred at the protein level. Western blotting analysis revealed a reduced expression of nNOS in SH-SY5Y cells at 48 h post transfection in comparison with the control group (Fig. 6a). The final in vitro assay examined the functionality of nNOS-targeted siRNAs regarding the viability of cells under injury. We found that nNOS-targeted siRNAs reduced the vulnerability of dopaminergic SH-SY5Y cells to 6-OHDA, the same neurotoxin also used to induce parkinsonism in animals. Transfecting cells with nNOS-targeted siRNAs reduced by 9.1% the toxicity caused by 6-OHDA on SH-SY5Y cells ($P < 0.05$; Fig. 6b).

**Table 2** Position of siRNA target sequences in rat and human nNOS mRNA

| nNOS coding exon | Position in rat NM_052799.1 and human NM_000620.4 | siRNA name | nNOS mRNA target sequence 5′–3′ |
|---|---|---|---|
| 2 | 767–787 | siRNAnNOSrat_767 | ACCAGCCAAAGCAGAGAUGAA |
| | 1392–1412 | siRNAnNOShum_767 | ACC**U**GCCAA**G**GCAGAGAUGAA |
| 12 | 2063–2083 | siRNAnNOSrat_2063 | CACGGAGUCCUUCAUCAAACA |
| | 2688–2708 | siRNAnNOShum_2063 | CAC**C**GAGUCCUUCAU**U**AA**G**CA |
| 25 | 3987–4007 | siRNAnNOSrat_3987 | CAGCGACAAUUUGACAUCCAA |
| | 4510–4530 | siRNAnNOShum_3987 | CAGCG**G**CAAUUUGA**U**AUCCAA |
| 28 | 4400–4420 | siRNAnNOSrat_4400 | CAGAACGUAUGAAGUGACCAA |
| | 4923–4943 | siRNAnNOShum_4400 | **GC**GAACGUA**C**GAAGUGACCAA |

Features of siRNAs targeting the rat and human nNOS mRNA. Mutated nucleotides between these species are in bold and underlined

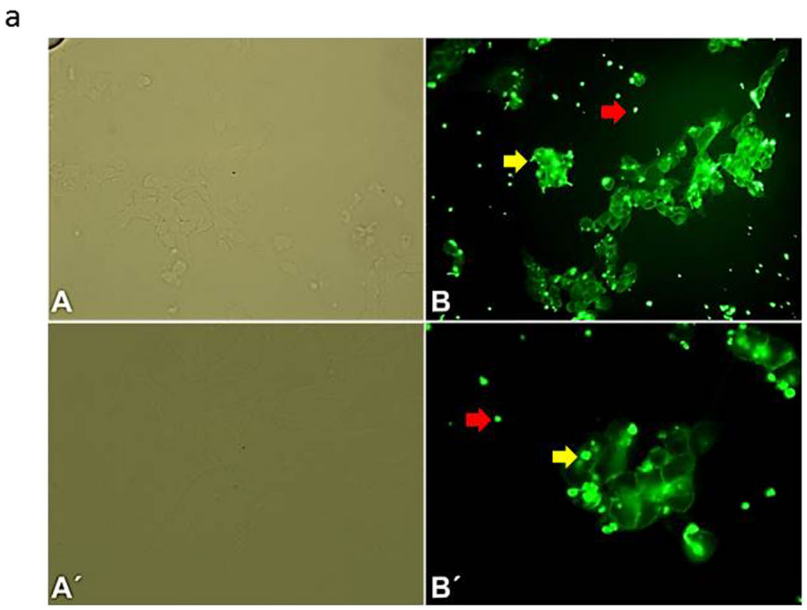


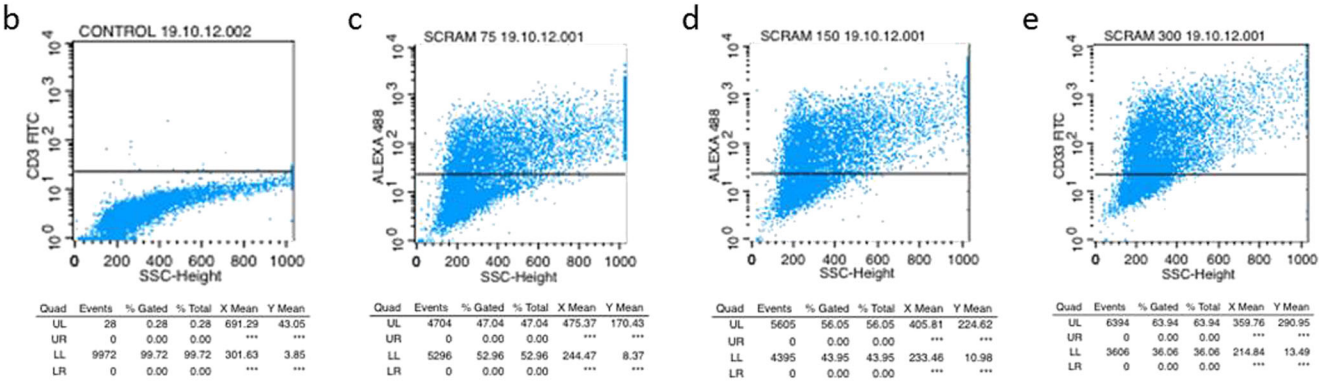


**Fig. 4** Transfection of labeled siRNAs in SH-SY5Y cells. **a** (A, A′) SH-SY5Y cells transfected with lipofectamine without Alexafluor 488-labeled siRNAs at 400× (A) and 1000× (A′) magnification, as a negative control group. **a** (B, B′) SH-SY5Y cells transfected with Alexafluor 488-labeled siRNAs, either internalized by cells (yellow arrow) or extracellular (red arrow), at 400× (B) and 1000× (B′) magnification. **b–e** Quantification of siRNA transfection by flow cytometry for siRNAnNOSrat_4400 at 75 pmol (**c**), 150 pmol (**d**), or 300 pmol (**e**); **b** control

## Intra-striatal Injection of nNOS-Targeted siRNAs Protected Nigral Cells from 6OHDA Injury

Injection of 6-OHDA in the rat striatum reproduced the key pathological process of Parkinson's disease, i.e., the loss of nigrostriatal dopaminergic neurons. Injured animals showed a marked reduction in TH-immunoreactivity in the substantia nigra ipsilateral to 6-OHDA injection (Fig. 7d). Pretreatment with siRNA_4400 at 4 days prior the lesion caused a significant improvement in TH-positive cells in comparison with scramble- and vehicle controls (Fig. 7f vs. 7e and d). TH immunoreactivity was quantified by densitometry in dorsal, lateral and ventral regions of the substantia nigra. Intrastriatal injections of siRNA_4400 caused a superior TH-labeling in all areas compared to scramble; the difference was statistically significant in substantia nigra dorsal and ventral (Fig. 7a, c; $P < 0.05$). Treatment with scrambled siRNAs caused no positive effects on dorsal and lateral regions and even potentiated the loss of TH-positive cells triggered by 6-OHDA in ventral region (Fig. 7c; $P < 0.05$). Altogether, those results show that nNOS-targeted siRNAs can control the injury of dopaminergic cells, making them less vulnerable to chemical injury.

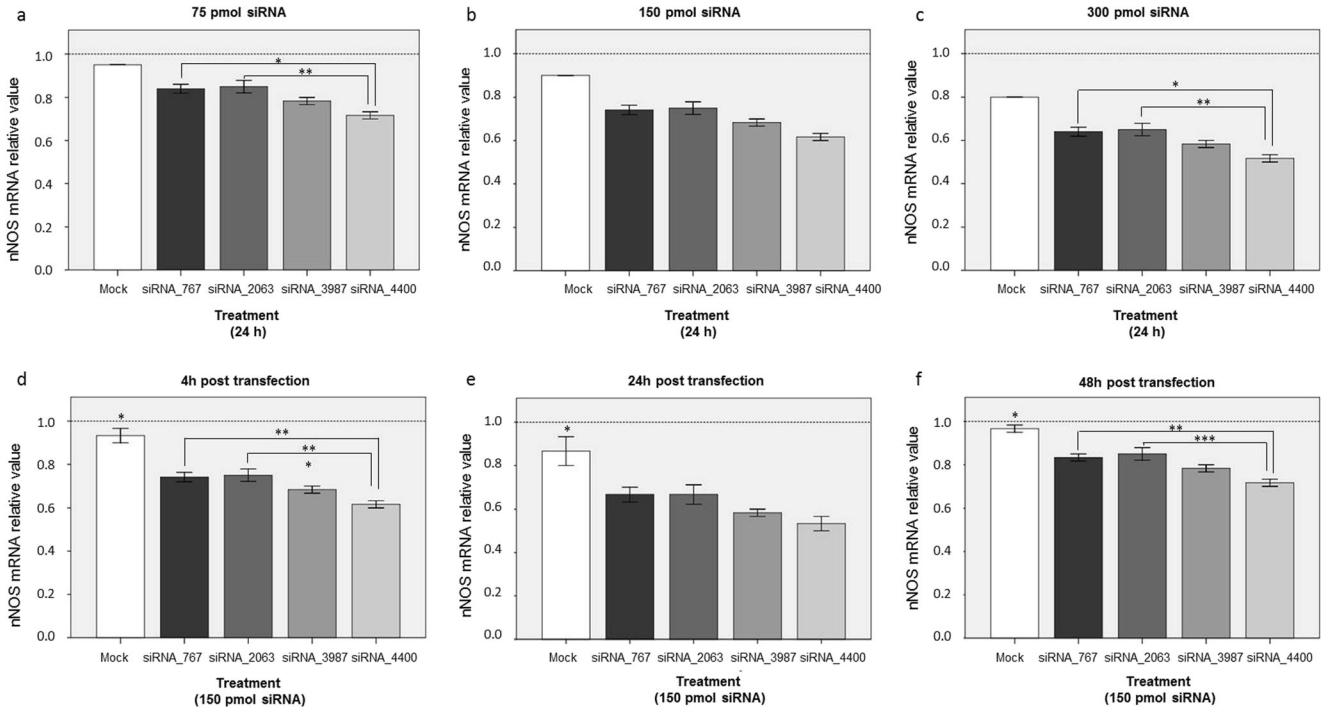


**Fig. 5** Knocking down of nNOS mRNA in SH-SY5Y cells. nNOS mRNA content was quantified by qPCR in cells transfected with siRNAs at three concentrations and time points. **a–c** nNOS mRNA decreased significantly after treatment with 75, 150, or 300 pmol of siRNA 4400 compared to siRNA_767 and 2063 (*$p < 0.05$, siRNA 767 vs. 4400; **$p < 0.05$, siRNA 2063 vs. 4400; ANOVA one-way followed by Tukey's post hoc). **d**, **f** nNOS mRNA content in cells transfected with 75 pmol of siRNA 4400 decreased significantly after 4 h and 48 h compared with siRNA 767 and 2063 (*$p < 0.05$, siRNA 767 vs. 4400; **$p < 0.05$, siRNA 2063 vs. 4400; ANOVA one-way followed by Tukey's post hoc). **e** Cells transfected with 75 pmol of siRNA 4400 at 24 h tended to show a decreased nNOS mRNA content compared with siRNA 767 and 2063

### Apomorphine-Induced Rotation Is Reduced in siRNA-Treated Animals

First, 6-OHDA injured animals showed an increased number of contralateral rotations induced by apomorphine, indicating a successful degeneration of nigrostriatal pathway. Pretreating animals with siRNA 4400 significantly reduced the number of turns (Fig. 8). This behavioral result agreed with the increased number of TH-positive nigral cells in siRNA_4400 treated animals (see Fig. 7).

## Discussion

The present study reveals that siRNA 4400, which triggered a knockdown of nNOS mRNA and protein, reduced the cytotoxicity caused by 6-OHDA on SH-SY5Y cells, as determined by MTT assay. Intra-striatal injection of the same duplex decreased the apomorphine-induced rotations and protected nigral TH(+) neurons in 6-OHDA hemi-lesioned rats.

PD is an age-related disorder characterized by progressive degeneration of dopaminergic neurons in the substantia nigra resulting in resting tremor, rigidity, bradykinesia or slowness, gait disturbance and postural instability (Przedborski 2005). Markers of oxidative stress, such as products of lipid peroxidation and oxidation of mitochondrial DNA and cytoplasmic RNA, are increased in dopaminergic neurons of PD brains (Dexter et al. 1989; Gaki and Papavassiliou 2014).

SH-SY5Y cell lineage is a compelling in vitro model of a dopaminergic neuron (Presgraves et al. 2004; Xicoy et al. 2017; Xie et al. 2010). Cells display characteristic markers of dopaminergic phenotype, including the expression of TH, dopamine-beta-hydroxylase, and the dopamine transporter (Agholme et al. 2010; Alberio et al. 2012; Cheung et al. 2009). In our study, we confirmed by immunocytochemistry that all SH-SY5Y cells were TH-positive. Then, this dopaminergic phenotype was confirmed by WB assay, which revealed a TH signal with the expected molecular size, similar to present in rat mesencephalic samples. Corroborating previous studies, differentiation with retinoic acid increased TH expression in SH-SY5Y cells. A very recent systematic review reported that less than 20% of studies with SH-SY5Y had employed forced differentiation (Xicoy et al. 2017). Furthermore, the use of retinoic acid in studies on neurodegeneration requires a careful interpretation of data, as it changes the effects of neurotoxins—including 6-OHDA—and proteasome inhibitors on SH-SY5Y (Cheng et al. 2013; Cheung et al. 2009; Lopes et al. 2010). Thus, we avoided forced differentiation of SH-SY5Y cells in experimental assays with 6-OHDA.

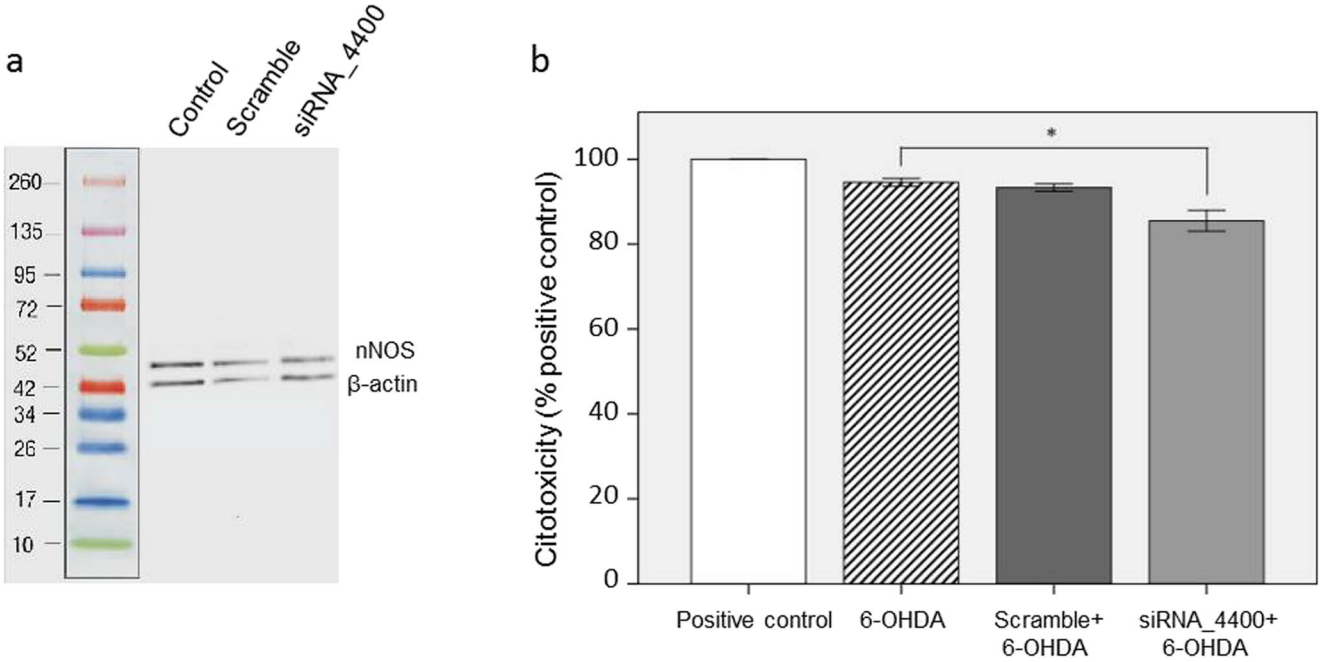


**Fig. 6** Silencing nNOS proteins and effects on the viability of injured cells. **a** Downregulation of nNOS protein by siRNA 4400 in comparison with control scramble and sham-transfected group, as revealed by Western blotting assay. **b** Neuroprotective effect of siRNA 4400, as shown by a significant reduction in 6-OHDA-induced cytotoxicity in SH-SY5Y cells ($P < 0.05$)

Finding mRNA sequences for RNAi is a critical step in assays with siRNA-mediated gene silencing (Titze-de-Almeida et al. 2017). The BIOPREDsi algorithm used in our work successfully predicted functional nNOS-target sequences, confirming previous results on target finder performance (Huesken et al. 2005; Matveeva et al. 2007). Indeed,

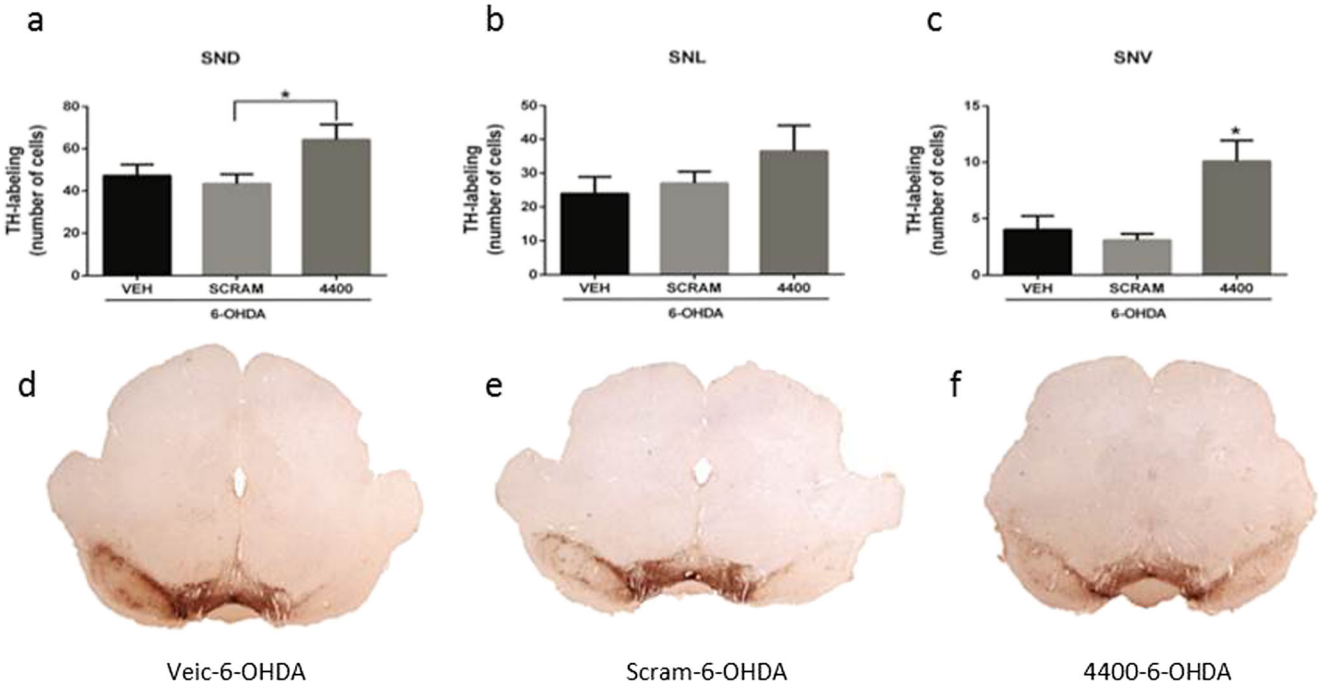


**Fig. 7** Neuroprotection of nigral dopaminergic neurons by siRNA 4400. **d–f** Brain coronal sections from rats injured with 6-OHDA showing TH(+) neurons of substantia nigra. **a–c** Densitometry analysis of TH-positive cells in substantia nigra dorsal (SND), lateral (SNL) and ventral (SNV) reveals an increased number of TH (+) cells in siRNA 4400-treated groups (4400, for simplicity), in SND and SNV, compared to scramble (SCRAM) and vehicle (VEH) groups. At day − 4 to 6-OHDA lesion, animals received the following intra-striatal injections: **d** vehicle; **e** siRNA scramble; **f** siRNA 4400. Compared to vehicle, pretreatment with siRNA 4400 reduced the loss of TH(+) cells caused by 6-OHDA in ipsilateral lesioned region

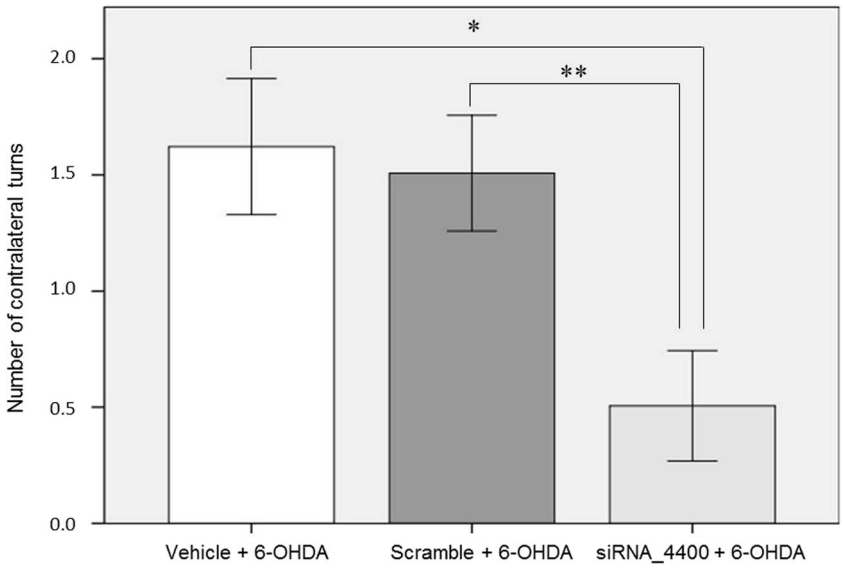


**Fig. 8** Reduction in rotation behavior by siRNA 4400. Intrastriatal injection of siRNA 4400 in 6-OHDA-injured animals caused a significant behavioral improvement, as revealed by a log decrease in contralateral turns induced by apomorphine in comparison with scrambled- and sham-treated groups ($P < 0.05$)

the proposed seven rules for examining each BIOPREDsi sequence also contributed for choosing nNOS-targeted siRNAs (Birmingham et al. 2007; Hajeri and Singh 2009; Reynolds et al. 2004; Vert et al. 2006). Theoretical prediction by target finders parallels only partially with the knock-down activity of siRNAs (Birmingham et al. 2007), a concern that we have reported in previous work (Cunha et al. 2013; Titze-de-Almeida et al. 2014). siRNA 4400 received the 4th BIOPREDsi score (0.87) but showed the highest nNOS silencing activity, followed by the best-scored siRNA 3987 (0.89).

Although all NOS forms can be found in the central nervous system, because of the temporal and spatial properties, the specific actions on neurotransmission can be attributed primarily to NO produced by nNOS (Kiss and Vizi 2001). Regarding siRNA 767, it targets all variants except nNOS gamma—a cytosolic protein that lacks the PDZ domain in exon 2 that docks nNOS protein to NMDA receptor. This siRNA presented the lowest silencing activity, suggesting that this variant was preserved and contributed to maintaining the content of nNOS mRNA. However, we cannot rule out that this reduced functionality of siRNA 767 could be a consequence of its low BIOPREDsi score (8th score; 0.86). Silencing effects were dose-dependent and significant yet at 4 h after transfection. Knockdown on nNOS peaked at 24 h after transfection, then showed a reduction at 48 h. This early but transient siRNA activity was previously reported with duplexes that share the same constitution but acting on other targets (Weber et al. 2006). Advances in oligonucleotides chemical structure now available have provided an extended duration of siRNA effects (Titze-de-Almeida et al. 2017).

Oxidative stress exerts a critical role in the loss of dopaminergic cells during PD progression (Antonelli et al. 2012; Hunot et al. 1996; Przedborski 2005). NO produced by NOS enzymes increases the levels of ROS, which causes oxidative stress and neuronal injury (Moncada and Bolanos 2006). Conversely, inhibition of NOS is neuroprotective. The preferential nNOS inhibitor 7-NI attenuated motor impairments and restored dopamine levels in female rats with bilateral intraventricular injection of 6-OHDA (Kumari et al. 2015). Our group and others reported that NOS inhibition with NOARG reverts 6-OHDA-induced striatal lesion (Gomes et al. 2008; Haik et al. 2008; Kumari et al. 2015). Indeed, 7-NI mitigates the dyskinesia induced by L-DOPA in unilaterally 6-OHDA-lesioned rats (Bortolanza et al. 2016; Del-Bel et al. 2014; Padovan-Neto et al. 2015; Padovan-Neto et al. 2009; Padovan-Neto et al. 2013; Solis et al. 2015). Finally, we found that both L-NAME or 7-NI counteracted the oxidative stress and apoptosis triggered by the neurotoxin MPP(+) in SH-SY5Y cells (Titze-de-Almeida et al. 2014). Most RNAi products in clinical testing are synthetic siRNAs, which reinforce the therapeutic potential of short RNA duplexes for different diseases, targets, and routes of administration (Titze-de-Almeida et al. 2017).

The discovery of a drug capable of preventing the loss of dopaminergic neurons in a parkinsonian brain is a matter of capital importance in neurology (Valera and Masliah 2016). Patients still have ≈ half of the nigrostriatal neurons viable and suffer from a relatively mild motor deficit in the early phase of disease, meaning that a "disease-modifying drug" for slowing down PD progression is of inestimable clinical value (Fahn 2018). Suppressing pathogenic proteins linked to neurodegeneration by RNAi is thus a strategic approach with potential neuroprotective effect (Bobbin and Rossi 2016; Smith and Zain 2019). And any toxic protein can be silenced by siRNAs, as the mechanism of action depends on Watson & Crick's base-pairing (Meister and Tuschl 2004). Finally, synthetic siRNAs are druggable, with at least ten products in

phases 2–3 clinical trials (Titze-de-Almeida et al. 2017). The first one fully translated to clinics was Patisiran (Onpattro™), a synthetic siRNA for Hereditary Transthyretin Amyloidosis approved by FDA in 2018 (Adams et al. 2018; Ledford 2018).

While silencing pathogenic proteins by siRNAs represents a wide avenue for drug development, it projects increased challenges in the field of neurological diseases. First, PD is a neurological disorder with prolonged duration (> 10 years) thereby requiring a drug with a sustainable therapeutic effect (Kalia and Lang 2015; Kempster et al. 2010). RNAi-based oligonucleotides now have an improved chemical structure (Ku et al. 2016). Ribose changes resulting in locked nucleic acids (LNA) and the substitution of a phosphodiester for a phosphorothioate bond between nucleotides are examples of chemical evolution incorporated in siRNAs with increased stability and specificity (Elmen et al. 2005; Khvorova and Watts 2017). For providing a sustainable delivery of siRNAs, a previous work complexed the oligonucleotides with PLGA polymers for intratumor injection, a technology that might be adapted for brain administration in chronic neurodegenerative diseases (Ramot et al. 2016).

Nanotechnology may also improve brain penetrance of siRNAs across the blood-brain barrier (Mathupala 2009; Pardridge 2007), as some therapeutics for neurological diseases failed because of this organic phase separation (de Boer and Gaillard 2007). Indeed, polymeric nanoparticles were developed for transfection of oligos into neuron cells (Soto-Sanchez et al. 2015). New carriers for PD show promising results for further clinical testing of siRNA-based therapies (Helmschrodt et al. 2017; Niu et al. 2017). Our group recently showed that Neuromag®, a magnetic particle composed by polystyrene copolymers and coated with iron, are capable of carrying and transfecting miRNA-target oligonucleotides into striatal neurons (Titze de Almeida et al. 2018). Furthermore, we obtained a significant target suppression effect in striatal cells after injecting the complex into the lateral ventricle. Such route of administration is of value for increased distribution of oligos in the striatum that is a brain structure next to the cerebral ventricle and anatomically extended across the rostrocaudal direction. Translating this strategy for patient therapy would also require stereotaxic surgery, along with methods for drug administration. In such sense, catheters or stents employed for brain injections by convection-enhanced delivery (CED), in association with nanoparticulated RNAi molecules, have shown efficacy in treating brain tumors, thereby they would be further exploited for a siRNA-based treatment of PD (Cohen et al. 2015; Lonser et al. 2015).

In conclusion, suppression of nNOS enzyme is thus a promising strategy to counteract the loss of dopaminergic neurons in PD. nNOS-targeted siRNAs represent an innovative approach for neuroprotection of dopaminergic cells and merit further pre-clinical testing as a disease-modifying agent for PD.

**Funding Information** This publication was funded by Fundação de Amparo a Pesquisa do Estado de São Paulo (FAPESP); Conselho Nacional de Desenvolvimento Científico e Tecnológico (CNPq; award number 467467/2014-5); Coordenação de Aperfeiçoamento de Pessoal de Nível Superior (CAPES; award number PNPD 0299081/2010 and PNPD 3731-37/2010); Fundação de Apoio a Pesquisa do Distrito Federal (FAPDF; award number 0193.001009/2015) and Instituto Nacional de Ciência e Tecnologia (INCT).

## References

Adams D, Gonzalez-Duarte A, O'Riordan WD, Yang CC, Ueda M, Kristen AV, Tournev I, Schmidt HH, Coelho T, Berk JL, Lin KP, Vita G, Attarian S, Planté-Bordeneuve V, Mezei MM, Campistol JM, Buades J, Brannagan TH III, Kim BJ, Oh J, Parman Y, Sekijima Y, Hawkins PN, Solomon SD, Polydefkis M, Dyck PJ, Gandhi PJ, Goyal S, Chen J, Strahs AL, Nochur SV, Sweetser MT, Garg PP, Vaishnaw AK, Gollob JA, Suhr OB (2018) Patisiran, an RNAi therapeutic, for hereditary transthyretin amyloidosis. N Engl J Med 379:11–21. https://doi.org/10.1056/NEJMoa1716153

Agholme L, Lindstrom T, Kagedal K, Marcusson J, Hallbeck M (2010) An in vitro model for neuroscience: differentiation of SH-SY5Y cells into cells with morphological and biochemical characteristics of mature neurons. J Alzheimers Dis 20:1069–1082. https://doi.org/10.3233/JAD-2010-091363

Alberio T, Lopiano L, Fasano M (2012) Cellular models to investigate biochemical pathways in Parkinson's disease. FEBS J 279:1146–1155. https://doi.org/10.1111/j.1742-4658.2012.08516.x

Alderton WK, Cooper CE, Knowles RG (2001) Nitric oxide synthases: structure, function and inhibition. Biochem J 357:593–615

Antonelli MC, Guillemin GJ, Raisman-Vozari R, del-Bel EA, Aschner M, Collins MA, Tizabi Y, Moratalla R, West AK (2012) New strategies in neuroprotection and neurorepair. Neurotox Res 21:49–56. https://doi.org/10.1007/s12640-011-9265-8

Birmingham A, Anderson E, Sullivan K, Reynolds A, Boese Q, Leake D, Karpilow J, Khvorova A (2007) A protocol for designing siRNAs with high functionality and specificity. Nat Protoc 2:2068–2078. https://doi.org/10.1038/nprot.2007.278

Bobbin ML, Rossi JJ (2016) RNA interference (RNAi)-based therapeutics: delivering on the promise? Annu Rev Pharmacol Toxicol 56:103–122. https://doi.org/10.1146/annurev-pharmtox-010715-103633

Bortolanza M, Bariotto-Dos-Santos KD, Dos-Santos-Pereira M, da-Silva CA, Del-Bel E (2016) Antidyskinetic effect of 7-Nitroindazole and sodium nitroprusside associated with amantadine in a rat model of Parkinson's disease. Neurotox Res 30:88–100. https://doi.org/10.1007/s12640-016-9618-4

Brown GC (2010) Nitric oxide and neuronal death. Nitric Oxide 23:153–165. https://doi.org/10.1016/j.niox.2010.06.001

Calabrese V, Mancuso C, Calvani M, Rizzarelli E, Butterfield DA, Stella AM (2007) Nitric oxide in the central nervous system: neuroprotection versus neurotoxicity. Nat Rev Neurosci 8:766–775. https://doi.org/10.1038/nrn2214

Castania V, Issy AC, Silveira JW, Ferreira FR, Titze-de-Almeida SS, Resende FFB, Ferreira NR, Titze-de-Almeida R, Defino HLA, del Bel E (2017) The presence of the neuronal nitric oxide synthase isoform in the intervertebral disk. Neurotox Res 31:148–161. https://doi.org/10.1007/s12640-016-9676-7

Cheng B, Martinez AA, Morado J, Scofield V, Roberts JL, Maffi SK (2013) Retinoic acid protects against proteasome inhibition associated cell death in SH-SY5Y cells via the AKT pathway. Neurochem Int 62:31–42. https://doi.org/10.1016/j.neuint.2012.10.014

Cheung YT, Lau WK, Yu MS, Lai CS, Yeung SC, So KF, Chang RC (2009) Effects of all-trans-retinoic acid on human SH-SY5Y neuroblastoma as in vitro model in neurotoxicity research.

Neurotoxicology 30:127–135. https://doi.org/10.1016/j.neuro.2008.11.001

Cohen ZR, Ramishetti S, Peshes-Yaloz N, Goldsmith M, Wohl A, Zibly Z, Peer D (2015) Localized RNAi therapeutics of chemoresistant grade IV glioma using hyaluronan-grafted lipid-based nanoparticles. ACS Nano 9:1581–1591. https://doi.org/10.1021/nn506248s

Cunha LC, Del Bel E, Pardo L, Stuhmer W, Titze DEAR (2013) RNA interference with EAG1 enhances interferon gamma injury to glioma cells in vitro. Anticancer Res 33:865–870

de Boer AG, Gaillard PJ (2007) Drug targeting to the brain. Annu Rev Pharmacol Toxicol 47:323–355. https://doi.org/10.1146/annurev.pharmtox.47.120505.105237

Del Bel EA et al (2005) Role of nitric oxide on motor behavior. Cell Mol Neurobiol 25:371–392

Del-Bel E, Padovan-Neto FE, Raisman-Vozari R, Lazzarini M (2011) Role of nitric oxide in motor control: implications for Parkinson's disease pathophysiology and treatment. Curr Pharm Des 17:471–488

Del-Bel E et al (2014) Counteraction by nitric oxide synthase inhibitor of neurochemical alterations of dopaminergic system in 6-OHDA-lesioned rats under L-DOPA treatment. Neurotox Res 25:33–44. https://doi.org/10.1007/s12640-013-9406-3

Dexter DT, Carter CJ, Wells FR, Javoy-Agid F, Agid Y, Lees A, Jenner P, Marsden CD (1989) Basal lipid peroxidation in substantia nigra is increased in Parkinson's disease. J Neurochem 52:381–389

Dotsch J, Harmjanz A, Christiansen H, Hanze J, Lampert F, Rascher W (2000) Gene expression of neuronal nitric oxide synthase and adrenomedullin in human neuroblastoma using real-time PCR. Int J Cancer 88:172–175

Douhou A et al (2002) Effect of chronic treatment with riluzole on the nigrostriatal dopaminergic system in weaver mutant mice. Exp Neurol 176:247–253

Dunkel P, Chai CL, Sperlagh B, Huleatt PB, Matyus P (2012) Clinical utility of neuroprotective agents in neurodegenerative diseases: current status of drug development for Alzheimer's, Parkinson's and Huntington's diseases, and amyotrophic lateral sclerosis. Expert Opin Investig Drugs 21:1267–1308. https://doi.org/10.1517/13543784.2012.703178

Ebadi M, Sharma SK (2003) Peroxynitrite and mitochondrial dysfunction in the pathogenesis of Parkinson's disease. Antioxid Redox Signal 5:319–335. https://doi.org/10.1089/152308603322110896

Elmen J et al (2005) Locked nucleic acid (LNA) mediated improvements in siRNA stability and functionality. Nucleic Acids Res 33:439–447. https://doi.org/10.1093/nar/gki193

Fahn S (2018) The 200-year journey of Parkinson disease: reflecting on the past and looking towards the future. Parkinsonism Relat Disord 46(Suppl 1):S1–S5. https://doi.org/10.1016/j.parkreldis.2017.07.020

Fire A, Xu S, Montgomery MK, Kostas SA, Driver SE, Mello CC (1998) Potent and specific genetic interference by double-stranded RNA in Caenorhabditis elegans. Nature 391:806–811. https://doi.org/10.1038/35888

Gaki GS, Papavassiliou AG (2014) Oxidative stress-induced signaling pathways implicated in the pathogenesis of Parkinson's disease. NeuroMolecular Med 16:217–230. https://doi.org/10.1007/s12017-014-8294-x

Gomes MZ, Del Bel EA (2003) Effects of electrolytic and 6-hydroxydopamine lesions of rat nigrostriatal pathway on nitric oxide synthase and nicotinamide adenine dinucleotide phosphate diaphorase. Brain Res Bull 62:107–115

Gomes MZ, Raisman-Vozari R, Del Bel EA (2008) A nitric oxide synthase inhibitor decreases 6-hydroxydopamine effects on tyrosine hydroxylase and neuronal nitric oxide synthase in the rat nigrostriatal pathway. Brain Res 1203:160–169. https://doi.org/10.1016/j.brainres.2008.01.088

Grant MK, Cuadra AE, El-Fakahany EE (2002) Endogenous expression of nNOS protein in several neuronal cell lines. Life Sci 71:813–817

Haik KL, Shear DA, Hargrove C, Patton J, Mazei-Robison M, Sandstrom MI, Dunbar GL (2008) 7-nitroindazole attenuates 6-hydroxydopamine-induced spatial learning deficits and dopamine neuron loss in a presymptomatic animal model of Parkinson's disease. Exp Clin Psychopharmacol 16:178–189. https://doi.org/10.1037/1064-1297.16.2.178

Hajeri PB, Singh SK (2009) siRNAs: their potential as therapeutic agents–part I. Designing of siRNAs. Drug Discov Today 14:851–858. https://doi.org/10.1016/j.drudis.2009.06.001

Hara MR, Snyder SH (2007) Cell signaling and neuronal death. Annu Rev Pharmacol Toxicol 47:117–141. https://doi.org/10.1146/annurev.pharmtox.47.120505.105311

Helmschrodt C, Höbel S, Schöniger S, Bauer A, Bonicelli J, Gringmuth M, Fietz SA, Aigner A, Richter A, Richter F (2017) Polyethylenimine nanoparticle-mediated siRNA delivery to reduce alpha-Synuclein expression in a model of Parkinson's disease. Mol Ther Nucleic Acids 9:57–68. https://doi.org/10.1016/j.omtn.2017.08.013

Herbison AE, Simonian SX, Norris PJ, Emson PC (1996) Relationship of neuronal nitric oxide synthase immunoreactivity to GnRH neurons in the ovariectomized and intact female rat. J Neuroendocrinol 8:73–82

Huesken D, Lange J, Mickanin C, Weiler J, Asselbergs F, Warner J, Meloon B, Engel S, Rosenberg A, Cohen D, Labow M, Reinhardt M, Natt F, Hall J (2005) Design of a genome-wide siRNA library using an artificial neural network. Nat Biotechnol 23:995–1001. https://doi.org/10.1038/nbt1118

Hunot S, Boissiere F, Faucheux B, Brugg B, Mouatt-Prigent A, Agid Y, Hirsch EC (1996) Nitric oxide synthase and neuronal vulnerability in Parkinson's disease. Neuroscience 72:355–363

Jimenez-Jimenez FJ, Alonso-Navarro H, Herrero MT, Garcia-Martin E, Agundez JA (2016) An update on the role of nitric oxide in the neurodegenerative processes of Parkinson's disease. Curr Med Chem 23:2666–2679

Kalia LV, Lang AE (2015) Parkinson's disease. Lancet 386:896–912. https://doi.org/10.1016/S0140-6736(14)61393-3

Kavya R, Saluja R, Singh S, Dikshit M (2006) Nitric oxide synthase regulation and diversity: implications in Parkinson's disease. Nitric Oxide 15:280–294. https://doi.org/10.1016/j.niox.2006.07.003

Kempster PA, O'Sullivan SS, Holton JL, Revesz T, Lees AJ (2010) Relationships between age and late progression of Parkinson's disease: a clinico-pathological study. Brain 133:1755–1762. https://doi.org/10.1093/brain/awq059

Khvorova A, Watts JK (2017) The chemical evolution of oligonucleotide therapies of clinical utility. Nat Biotechnol 35:238–248. https://doi.org/10.1038/nbt.3765

Kiss JP, Vizi ES (2001) Nitric oxide: a novel link between synaptic and nonsynaptic transmission. Trends Neurosci 24:211–215

Ku SH, Jo SD, Lee YK, Kim K, Kim SH (2016) Chemical and structural modifications of RNAi therapeutics. Adv Drug Deliv Rev 104:16–28. https://doi.org/10.1016/j.addr.2015.10.015

Kumari R, Kumar JB, Luthra PM (2015) Post-lesion administration of 7-NI attenuated motor and non-motor deficits in 6-OHDA induced bilaterally lesioned female rat model of Parkinson's disease. Neurosci Lett 589:191–195. https://doi.org/10.1016/j.neulet.2014.12.030

Kwon MJ, Oh E, Lee S, Roh MR, Kim SE, Lee Y, Choi YL, in YH, Park T, Koh SS, Shin YK (2009) Identification of novel reference genes using multiplatform expression data and their validation for quantitative gene expression analysis. PLoS One 4:e6162. https://doi.org/10.1371/journal.pone.0006162

Ledford H (2018) Gene-silencing technology gets first drug approval after 20-year wait. Nature 560:291–292. https://doi.org/10.1038/d41586-018-05867-7

Livak KJ, Schmittgen TD (2001) Analysis of relative gene expression data using real-time quantitative PCR and the 2(−Delta Delta C(T)) method. Method 25:402–408. https://doi.org/10.1006/meth.2001.1262

Lonser RR, Sarntinoranont M, Morrison PF, Oldfield EH (2015) Convection-enhanced delivery to the central nervous system. J Neurosurg 122:697–706. https://doi.org/10.3171/2014.10.JNS14229

Lopes FM, Schröder R, Júnior MLCF, Zanotto-Filho A, Müller CB, Pires AS, Meurer RT, Colpo GD, Gelain DP, Kapczinski F, Moreira JCF, Fernandes MC, Klamt F (2010) Comparison between proliferative and neuron-like SH-SY5Y cells as an in vitro model for Parkinson disease studies. Brain Res 1337:85–94. https://doi.org/10.1016/j.brainres.2010.03.102

Mathupala SP (2009) Delivery of small-interfering RNA (siRNA) to the brain. Expert Opin Ther Pat 19:137–140. https://doi.org/10.1517/13543770802680195

Matveeva O, Nechipurenko Y, Rossi L, Moore B, Saetrom P, Ogurtsov AY, Atkins JF, Shabalina SA (2007) Comparison of approaches for rational siRNA design leading to a new efficient and transparent method. Nucleic Acids Res 35:e63. https://doi.org/10.1093/nar/gkm088

Meister G, Tuschl T (2004) Mechanisms of gene silencing by double-stranded RNA. Nature 431:343–349. https://doi.org/10.1038/nature02873

Moncada S, Bolanos JP (2006) Nitric oxide, cell bioenergetics and neurodegeneration. J Neurochem 97:1676–1689. https://doi.org/10.1111/j.1471-4159.2006.03988.x

Mukherjee P, Cinelli MA, Kang S, Silverman RB (2014) Development of nitric oxide synthase inhibitors for neurodegeneration and neuropathic pain. Chem Soc Rev 43:6814–6838. https://doi.org/10.1039/c3cs60467e

Niu S, Zhang LK, Zhang L, Zhuang S, Zhan X, Chen WY, du S, Yin L, You R, Li CH, Guan YQ (2017) Inhibition by multifunctional magnetic nanoparticles loaded with alpha-Synuclein RNAi plasmid in a Parkinson's disease model. Theranostics 7:344–356. https://doi.org/10.7150/thno.16562

Padovan-Neto FE, Cavalcanti-Kiwiatkoviski R, Carolino RO, Anselmo-Franci J, Del Bel E (2015) Effects of prolonged neuronal nitric oxide synthase inhibition on the development and expression of L-DOPA-induced dyskinesia in 6-OHDA-lesioned rats. Neuropharmacology 89:87–99. https://doi.org/10.1016/j.neuropharm.2014.08.019

Padovan-Neto FE, Echeverry MB, Chiavegatto S, Del-Bel E (2011) Nitric oxide synthase inhibitor improves De novo and long-term l-DOPA-induced dyskinesia in Hemiparkinsonian rats. Front Syst Neurosci 5:40. https://doi.org/10.3389/fnsys.2011.00040

Padovan-Neto FE, Echeverry MB, Tumas V, Del-Bel EA (2009) Nitric oxide synthase inhibition attenuates L-DOPA-induced dyskinesias in a rodent model of Parkinson's disease. Neuroscience 159:927–935. https://doi.org/10.1016/j.neuroscience.2009.01.034

Padovan-Neto FE, Ferreira NR, de Oliveira-Tavares D, de Aguiar D, da Silva CA, Raisman-Vozari R, Del Bel E (2013) Anti-dyskinetic effect of the neuronal nitric oxide synthase inhibitor is linked to decrease of FosB/deltaFosB expression. Neurosci Lett 541:126–131. https://doi.org/10.1016/j.neulet.2013.02.015

Pardridge WM (2007) Blood-brain barrier delivery. Drug Discov Today 12:54–61. https://doi.org/10.1016/j.drudis.2006.10.013

Paxinos G, Watson C (2005) The Rat Brain in Stereotaxic Coordinates. 5th edn. Elsevier Academic Press, San Diego

Presgraves SP, Ahmed T, Borwege S, Joyce JN (2004) Terminally differentiated SH-SY5Y cells provide a model system for studying neuroprotective effects of dopamine agonists. Neurotox Res 5:579–598

Przedborski S (2005) Pathogenesis of nigral cell death in Parkinson's disease. Parkinsonism Relat Disord 11(Suppl 1):S3–S7. https://doi.org/10.1016/j.parkreldis.2004.10.012

Ramot Y, Rotkopf S, Gabai RM, Zorde Khvalevsky E, Muravnik S, Marzoli GA, Domb AJ, Shemi A, Nyska A (2016) Preclinical safety evaluation in rats of a polymeric matrix containing an siRNA drug used as a local and prolonged delivery system for pancreatic Cancer therapy. Toxicol Pathol 44:856–865. https://doi.org/10.1177/0192623316645860

Reynolds A, Leake D, Boese Q, Scaringe S, Marshall WS, Khvorova A (2004) Rational siRNA design for RNA interference. Nat Biotechnol 22:326–330. https://doi.org/10.1038/nbt936

Sales TT, Resende FF, Chaves NL, Titze-De-Almeida SS, Bao SN, Brettas ML, Titze-De-Almeida R (2016) Suppression of the Eag1 potassium channel sensitizes glioblastoma cells to injury caused by temozolomide. Oncol Lett 12:2581–2589. https://doi.org/10.3892/ol.2016.4992

Smith CIE, Zain R (2019) Therapeutic oligonucleotides: state of the art. Annu Rev Pharmacol Toxicol 59:605–630. https://doi.org/10.1146/annurev-pharmtox-010818-021050

Solis O, Espadas I, Del-Bel EA, Moratalla R (2015) Nitric oxide synthase inhibition decreases l-DOPA-induced dyskinesia and the expression of striatal molecular markers in Pitx3(−/−) aphakia mice. Neurobiol Dis 73:49–59. https://doi.org/10.1016/j.nbd.2014.09.010

Soto-Sanchez C, Martinez-Navarrete G, Humphreys L, Puras G, Zarate J, Pedraz JL, Fernandez E (2015) Enduring high-efficiency in vivo transfection of neurons with non-viral magnetoparticles in the rat visual cortex for optogenetic applications. Nanomedicine 11:835–843. https://doi.org/10.1016/j.nano.2015.01.012

Titze de Almeida SS, Horst CH, Soto-Sanchez C, Fernandez E, Titze de Almeida R (2018) Delivery of miRNA-targeted oligonucleotides in the rat striatum by Magnetofection with Neuromag((R)) Molecules 23 https://doi.org/10.3390/molecules23071825

Titze-de-Almeida R, David C, Titze-de-Almeida SS (2017) The race of 10 synthetic RNAi-based drugs to the pharmaceutical market. Pharm Res 34:1339–1363. https://doi.org/10.1007/s11095-017-2134-2

Titze-de-Almeida SS, Lustosa CF, Horst CH, Bel ED, Titze-de-Almeida R (2014) Interferon gamma potentiates the injury caused by MPP(+) on SH-SY5Y cells, which is attenuated by the nitric oxide synthases inhibition. Neurochem Res 39:2452–2464. https://doi.org/10.1007/s11064-014-1449-1

Valera E, Masliah E (2016) Therapeutic approaches in Parkinson's disease and related disorders. J Neurochem 139 Suppl 1:346–352. https://doi.org/10.1111/jnc.13529

Vert JP, Foveau N, Lajaunie C, Vandenbrouck Y (2006) An accurate and interpretable model for siRNA efficacy prediction. BMC Bioinformatics 7:520. https://doi.org/10.1186/1471-2105-7-520

Vistica DT, Skehan P, Scudiero D, Monks A, Pittman A, Boyd MR (1991) Tetrazolium-based assays for cellular viability: a critical examination of selected parameters affecting formazan production. Cancer Res 51:2515–2520

Weber C, Mello de Queiroz F, Downie BR, Suckow A, Stuhmer W, Pardo LA (2006) Silencing the activity and proliferative properties of the human EagI Potassium Channel by RNA interference. J Biol Chem 281:13030–13037. https://doi.org/10.1074/jbc.M600883200

Xicoy H, Wieringa B, Martens GJ (2017) The SH-SY5Y cell line in Parkinson's disease research: a systematic review. Mol Neurodegener 12:10. https://doi.org/10.1186/s13024-017-0149-0

Xie HR, Hu LS, Li GY (2010) SH-SY5Y human neuroblastoma cell line: in vitro cell model of dopaminergic neurons in Parkinson's disease. Chin Med J 123:1086–1092

Zhou L, Zhu DY (2009) Neuronal nitric oxide synthase: structure, subcellular localization, regulation, and clinical implications. Nitric Oxide 20:223–230. https://doi.org/10.1016/j.niox.2009.03.001

**Publisher's Note** Springer Nature remains neutral with regard to jurisdictional claims in published maps and institutional affiliations.